



BUDAPEST UNIVERSITY OF TECHNOLOGY AND ECONOMICS  
DEPARTMENT OF STRUCTURAL MECHANICS

## **BIOMECHANICAL MODELLING OF THE EYE**

Summary and Theses of PhD dissertation

**ZOLTÁN BOCSKAI**

Supervisor:  
**DR. IMRE BOJTÁR**

Budapest, 2015

## **Contents**

<b>1. Introduction</b>	<b>3</b>
<b>2. Methods and results</b>	<b>4</b>
2.1. Introduction of the purposes of the numerical calculations.....	4
2.1.1 The complex finite element model.....	5
2.1.2 Analysis of the accommodation amplitude.....	6
2.1.3 Numerical analysis of a non-refractive eye surgery.....	9
2.2 Experimental analysis of the zonular fibres.....	12
2.2.1 Measurement of the zonular geometry.....	12
2.2.2 Evaluation of the mechanical behaviour of the zonular fibres.....	12
<b>3. New scientific results</b>	<b>18</b>
<b>Publication on the subject of the dissertation</b>	<b>19</b>

## **1. Introduction**

Nowadays, the application of different ophthalmic procedures is the most ambitious and one of the most appropriate method to eliminate barriers to vision problems. The majority of these interventions require surgery, which expects depth of physiological and biomechanical knowledge about the properties of the eye. There are several ophthalmic surgeries which are able to eliminate various medical problems. One of these procedures is connected to the corneal surface, where the goal is to improve near, or far-sightedness (PRK, LASIK). Another surgical technique involving the sclera aims to restore the natural accommodation of the lens (LaseACE). Another important surgery type is the group of cataract surgeries in which the lens are replaced by intraocular lens (IOL). Based on the previous facts it seems especially useful to create a numerical model for the investigation of the above-mentioned problems from biomechanical point of view. In recent years, several studies have been made for the mechanical analysis of various parts of the eye. These problems were usually modelled by a computer program based on the finite element method. However, such a complex model is very rare that is suitable for a global analysis and detailed enough to deal with most of the biomechanical problems related to the eye. In most of the studies the different parts in the partial or slightly more complex models are characterized by homogeneous, isotropic and linear elastic material model. There are a few publications with nonlinear material models, but in these cases, the analyses were performed only on certain parts of the eye. This is so because to measure the material properties of the eye is extremely difficult. In addition, there is a lack of mechanical properties describing the linearly elastic behaviour. The reason of this is that the in vivo measurement of these parameters is almost impossible and in vitro measurements are still very cumbersome due to the structure of the eye. In contrast with the material properties, the determination of the geometrical dimensions can be treated as a solved problem, because the measurement of the anterior and posterior segment in vivo is possible by ophthalmic tools. In this dissertation, I deal with the complex three-dimensional finite element modelling of the eye, in particular focusing on the examination of accommodation. The thesis has been made in close cooperation with the Department of Ophthalmology at Semmelweis University. One of the targets of my work is to prepare, parametrize and test such a numerical model which is able to investigate the accommodation of the eye and also other numerical simulations (e.g. the analysis of mechanical behaviour of various eye surgery). My further purpose is the deeper understanding of the lens surrounding zonular fibres as well as the measurement of the material parameters. This induced the development of a specific experimental procedure, which can be performed in a reproducible manner to get the elastic properties of the fibres. The chapters in the thesis, after a short theoretical introduction, are the followings:

- creation of the complex model of the eye, including the important parts from biomechanical point of view
- detailed modelling of the lens and the surrounding parts
- demonstration of the model on examination of the accommodation
- clinical applications to modify the geometry of the surgical procedure which is able to restore the natural accommodation
- detailed review of the developed procedure made for the analysis of elastic properties of zonular fibres, evaluation of the experimental results

The chapters of the dissertation include the following:

*Complex finite element modelling of the eye*

The constituent parts of the eye are taken into account as homogeneous elastic continuum in the numerical investigations, whose geometrical and mechanical properties can be easily changed as needed in view of the real parameters. The applied parameters are partly originated from the specialized literature and partly from own experiments. The eye, as a living tissue, is continuously transforming during its lifetime. On one hand, the geometry of the lens is changing with maturing, on the other hand, the components of the eye are gradually stiffening, i.e. the modulus of elasticity increasing with the age. Moreover, the optical properties of the lens (such as refractive index) also vary. The structure of the developed algorithm connected to the complex model allows the flexible variation of the geometric and material parameters based on the measured, or the newly determined data.

*Modelling of the accommodation process*

With the complex numerical model, the accommodation of the lens is analyzed in the function of the age. The results are compared with clinical measurements to prove the applicability of the developed model. In addition, my simulations show that beside the geometric and material parameters the optical properties (refractive index) of the lens also affect the accommodation process.

*Analyzing the surgical method related to the sclera*

In order to increase the efficiency of the surgical procedure, a parametric study is performed using the finite element numerical model. This may assist in the improvement of the surgical procedure in order to increase the natural accommodation width of the eye.

*Laboratory measurements of the mechanical properties of the zonular fibres*

The zonular fibres strongly affect the mechanism of the lens accommodation, therefore a reproducible laboratory test is evolved to measure and evaluate the elastic parameters of the zonules. The most important characteristic of the laboratory test method is the in-situ measurement. For the quick evaluation of the experimental results analytical and numerical solutions are provided. The laboratory measurement method and the evaluation process is developed with the utilization of porcine samples, but the complete procedure can be adapted to human eyes.

## **2. Methods and results**

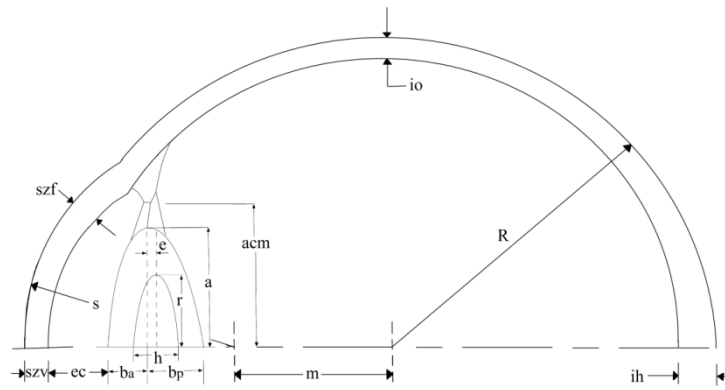
### **2.1. Introduction of the purposes of the numerical calculations**

The main goal of the numerical modelling is to create such a complex model that is suitable to analyze different kind of problems. For this purpose, the ANSYS program is utilized based on the finite element technique. For the sake of wide range of applicability, the model is three-dimensional. In this dissertation, it is used to investigate the **accommodation** of the lens and to **a surgical method which involving the sclera**. The model is verified with the analysis of the accommodation together with the factors affecting it. After these investigations, a surgical method is studied, where the basic idea is to create micro-excisions into the sclera (with ophthalmic laser) to restore the natural accommodation of the eye. Based on the analyzed geometry of the original surgery a possible new geometry is proposed, which is more powerful to reach wider accommodation width.

### 2.1.1 The complex finite element model

At the creation of the geometry the axisymmetric property of the eyeball is taken into account, but it is not valid and used for the surrounding fat (Fig. 1 and 2). The parametric design language (APDL) of ANSYS is applied, the main geometrical properties in the manner described below can be arbitrarily modified. For the construction of the geometry of the eyeball the following parameters can be used (Fig. 1):

- outer radius of the eyeball ( $R$ ),
- posterior ( $ih$ ) and side thickness ( $io$ ) of the sclera,
- outer radius of the cornea ( $s$ ),
- anterior ( $szv$ ) and side ( $szf$ ) thickness of the sclera,
- anterior chamber depth ( $ec$ ),
- the distance between the center of curvature of the eyeball and the cornea ( $m$ ),
- equatorial radius of the lens ( $a$ ),
- lens thickness ( $b=b_a+b_p$ ),
- parameters for the tendency of curvature of the lens ( $c, d$ ),
- thickness of the nucleus ( $h$ ),
- radius of the nucleus ( $r$ ),
- position of the nucleus respect to equator of the lens ( $e$ ),
- anterior capsular thickness ( $tva$ ) and posterior capsular thickness ( $tvp$ ),
- inner diameter of the ciliary body ( $acm$ ).



- Figure 1 – The geometrical parameters

The input file is created in such a way that the ANSYS program automatically generates the geometrical frame of the model based on the prescribed parameters. The eyeball is located in the orbit, inside the surrounding fatty tissue (Fig. 2). In the model, between the lens capsule, cortex, nucleus and the vitreous body a bonded connection is assumed because there is no information about the mechanical behaviour between the mentioned parts so far.

For the modelling of the lens capsule and the zonular apparatus shell finite elements are used, because these parts are extremely thin (6-60  $\mu\text{m}$ ). The rest of the constituents are modelled with solid elements (Fig. 2).

The great advantage of my model is that the modification of the input geometrical and material parameters is very simple. The applied values of these parameters in the numerical calculations is based on numerous literatures. (For details on these sources, see the relevant chapter of the dissertation.)

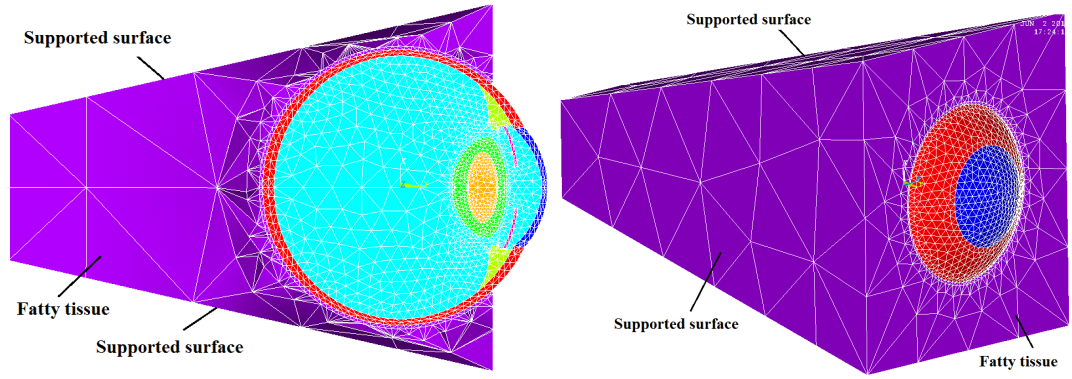


Figure 2 – The section of the numerical model and the fatty tissue with the boundary conditions

### 2.1.2 Analysis of the accommodation amplitude

For the analysis of the mechanism of the accommodation process, a radial force system is applied on the ciliary body that causes tension in the zonules (Fig. 3). In this way, the lens are deformed from the near seeing (accommodated) state to the far seeing (unaccommodated) state. The lens thickness becomes thinner under this process (Fig. 4), which is reasonable due to the fact that in the accommodated state the zonules and the lens are in stress free state. The translations are set to zero on the side panels of the fatty tissue (Fig. 2) to model the supporting effect of the orbit. To evaluate the accommodation mechanism, the calculation of the central optical power (*COP*) of the lens in the different ages in accommodated and in unaccommodated states is necessary. By this step, the thick lens formula is used to get the dioptr of the lens:

$$COP = \frac{n_l - n_p}{r_a} + \frac{n_l - n_p}{r_p} - \frac{t(n_l - n_p)^2}{r_a r_p n_l}, \quad (1)$$

where  $n_l$  is the equivalent refractive index of the lens respect to air (1.42 but this value depends on the age),  $n_p$  is the refractive index of the vitreous body and the aqueous humour (1.336),  $r_a$  and  $r_p$  are the radius of curvature at the anterior and posterior side of the lens in the symmetric axis and  $t$  is the thickness of the lens. To calculate the *COP* the determination of the radius of curvatures in the accommodated and in the unaccommodated state is needed.

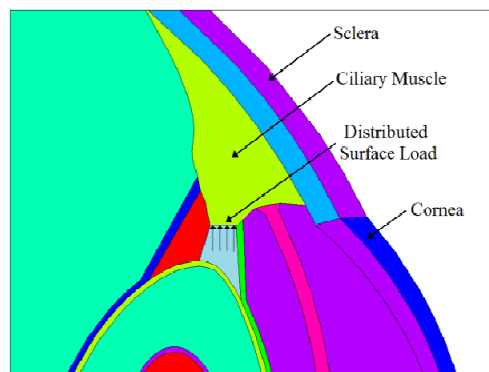


Figure 3 – The applied radial force system on the ciliary body

By this calculation, the nodal coordinates from the undeformed and deformed states are used for a polynomial regression at the outline of the symmetric plain of the lens. Those nodes are selected whose distance from the symmetric axis is maximum 3 mm. Due to the fact that the

deformed nodal coordinates are received from the finite element calculation, the function of the outline of the lens from which the radius of curvature could be calculated is unknown. For the elimination of this problem, the following method is used. Based on *Chien et al.* [2003] (Equation (2), where  $a$ ,  $b$ ,  $c$  and  $d$  are constants for the shape of the lens) the initial function of the shape of lens is known, and from this the function of the radius of curvature is known ( $r(x)$ ). Thus, different order of polynomials are fitted on the initial nodal coordinates of the outline of the lens with the application of the least squares method. From the different order polynomials, the function of the radius of curvature ( $r_{pol}(x)$ ) can be calculated.

$$y(x) = \left[ b + c \left( \sin^{-1} \left( \frac{x}{a} \right) \right)^2 + d \left( \sin^{-1} \left( \frac{x}{a} \right) \right)^4 \right] \cos \left( \sin^{-1} \left( \frac{x}{a} \right) \right), \quad (2)$$

Based on these two functions of radius of curvature, Equation (3) can be calculated. From the different order of polynomials, the one for which Equation (3) gives minimum (Fig. 5) is accepted as the best fitting polynomial.

$$\int_{-3mm}^{3mm} (r(x) - r_{pol}(x))^2 dx \rightarrow \min. \quad (3)$$

As a result of this process, we get the best-fitted order of polynomial on the original shape of the lens respect to the radius of curvature, and this order of polynomial is fitted on the deformed nodal coordinates. With the aim of these polynomials, the *COP* value and the accommodation amplitude ( $\Delta COP$  the difference between the *COP* in deformed and undeformed shape) are calculated.

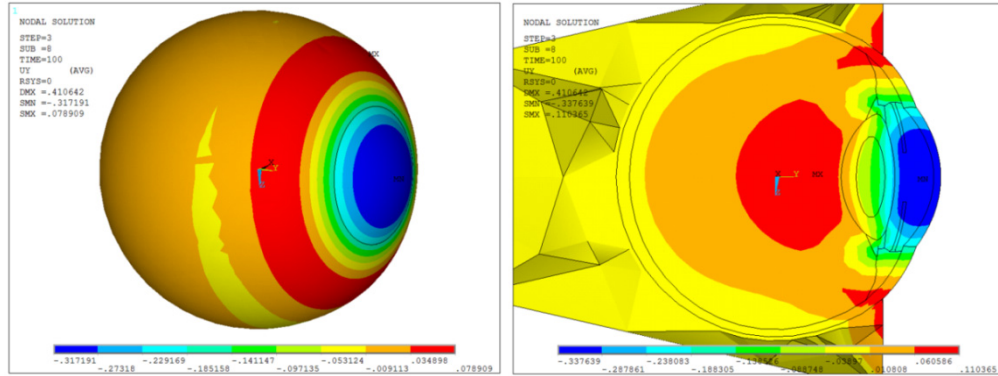


Figure 4 – The translations in the direction of the symmetric axis

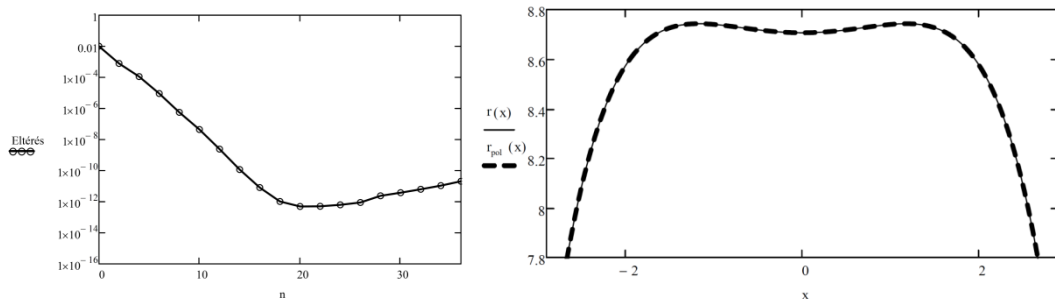


Figure 5 – The relative difference between the function of the radius of curvature from the original and from the fitted one in the function of the order of polynomials [ $n$ ]; the function of the radius of curvature from the original function of the lens ( $r(x)$ , [mm]) and from the fitted polynomials ( $r_{pol}(x)$ , [mm])

The amplitude of accommodation with ageing is analysed (for this calculation, see the applied material and geometrical parameters in the thesis). The central optical power is calculated in four different cases. In all four cases and in all ages the intensity of the stretching force was the same, but the material properties of the lens nucleus, cortex and capsule, and the thickness of the capsule are diverse in these periods. In the first case, it is assumed that the lens geometry and the refractive index of the lens are constant in all ages, so only the material parameters and the thickness of the lens capsule are the variables. In the second case, the geometry is the same in every age, but the variation of the refractive index and material properties are also taken into consideration. In the third case the geometry of the lens cortex and nucleus are age-related, but the refractive index remains constant, and in the fourth case both the lens geometry and the refractive index of the lens are age-related.

The *COP* of the lens is calculated both with the initial geometry and with the deformed shape (in accommodated and unaccommodated states). We can see the alteration of dioptré in accommodated and unaccommodated situations in all four analysed cases (Fig. 6).

In the first case, because the initial geometry (accommodated state) is the same in each analysed age, and the refractive index is constant, we can see different optical power only in unaccommodated states (as shown in Fig. 6). In the second one, we consider that the refractive index decreases with ageing, but the geometry is the same as in the previous case, so the dioptré of the lens in accommodated and unaccommodated states is smaller.

In the third case, we consider that the lens become thicker with ageing and its curvature is getting larger. According to Fig. 6, the dioptré of the lens increases during ageing in accommodated and unaccommodated states too (case 3).

In the fourth case, where the lens thickens and the refractive index decreases with ageing the optical power of the lens is calculated, and the results can be seen in Fig. 6. Now, according to the expectations, the initial values of dioptré are the same as in the third case, and the final values are the same as in second case.

With the results of the previous chapter, we can calculate the amplitude of accommodation if we subtract the dioptré of unaccommodated state from the dioptré of accommodated state. Based on the finite element and optical calculations, our numerical results in all examined cases confirm that the amplitude of accommodation ( $\Delta COP$ ) reduces with ageing (see Fig. 6).

Considering that the refractive index of the crystalline lens decreases with increasing age and the thickness of the lens is increasing with it the most accurate calculation is case four.

We can say that the amplitude of accommodation is getting worse if we consider the decreasing of the refractive index of the lens (case two and case four). The decreasing tendency of the amplitude of accommodation is based on numerical and optical calculations, and it is shown in Fig. 6. It has been demonstrated that beside the age-related material and geometric properties, the effect of the refractive index of the lens is also important (Fig. 6).

Fig. 6 also shows results for a fifth case, where based on *Śródka et al.* [2011] reduced elastic modulus is used for the sclera and cornea. Besides these changes, the decreasing of refractive index and the age-related material and geometric parameters are considered similarly to case four.

If we compare our numerical results with values measured by *Tsorbatzoglou et al.* (2007) based on defocusing technique, the following diagram can be obtained (see also Fig. 6). The numerical calculations and the measured results show good agreement in the tendency of the amplitude of the accommodation.

Based on this information, it can be established that at the analyses of accommodation, not only the age-related material and geometric properties, but also the age-related optical parameters are important with the same weight. It should be noted that in the calculation of

the central optical power only the effects of the lens, the vitreous body and the aqueous humour are considered, the refractive index of the lens is assumed constant along the optical axis.

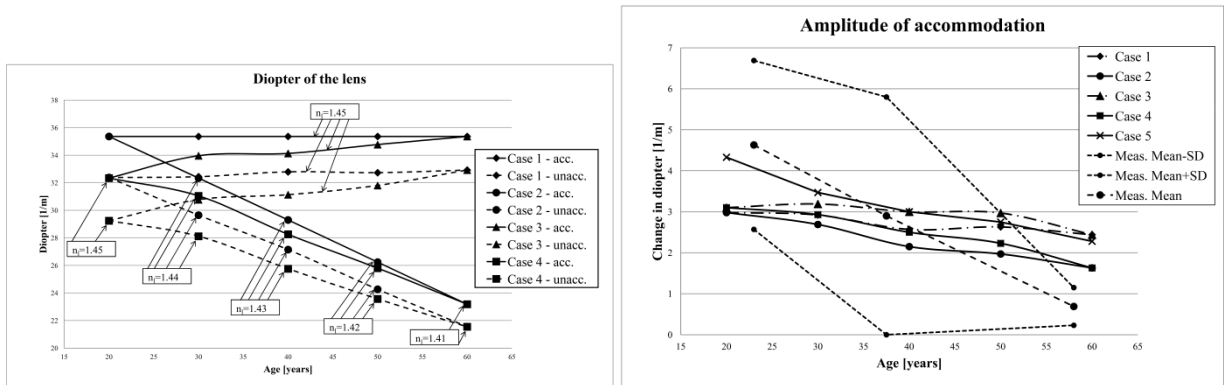


Figure 6 – The changing of the center optical power of the lens and the changing of the accommodation amplitude in the different cases as a function of age

### 2.1.3 Numerical analysis of a non-refractive eye surgery

In addition to the refractive surgery techniques, non-refractive ones also exist. *Hipsley and McDonald* [2012] demonstrated a new method connected with the sclera. With ophthalmic laser, they create micro-excisions into the sclera, which results the increasing of the accommodation amplitude with an average 1.3 dioptries value to treat presbyopia. This laser technology (*Hipsley and McDonald* [2012]) is a patented process. In the original geometry, the number of the micro-excisions is 36 and the diameter of them is 600  $\mu\text{m}$ . The depth of the micro-excisions in the sclera is 80-90% of its thickness (Fig. 7 and Fig. 8).

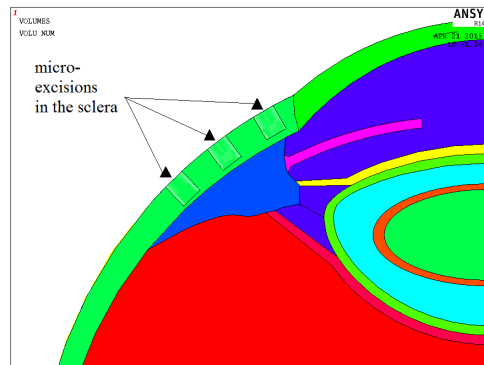


Figure 7 – Section of the model through the axis of the eyeball, showing the position and the depth of the micro-excisions in the sclera

The average residual increment of the accommodation width is 1.3 dioptries due to this surgical technique. They measured the accommodation width in an objective way. My purpose is to increase the efficiency of this surgical procedure and its mechanism by the modification of its original geometry. With the help of the former complex model, constant distributed load is applied on the ciliary body to analyze the variation in the accommodation width with different geometry and hole patterns of the surgery. As a result of this analysis, it has been proved that the amount of the volume of the micro holes and their position affect the accommodation width.

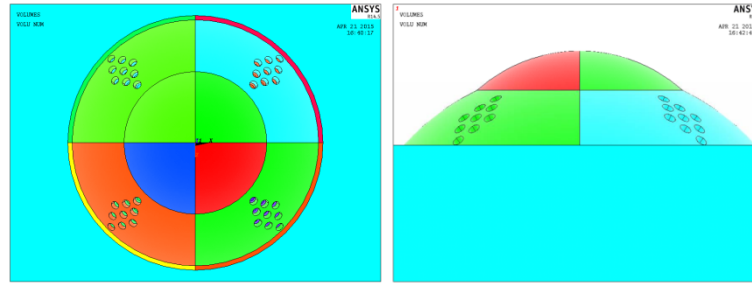


Figure 8 – The original geometry of the surgical procedure

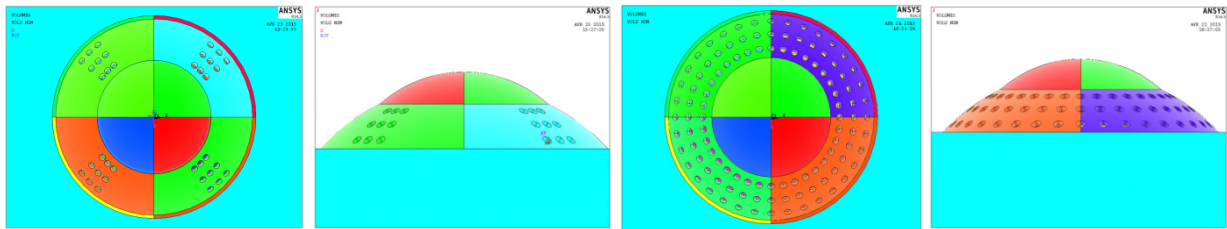


Figure 9 – The geometry of the concentrated and the continuous hole patterns

Theoretically, the efficiency of this laser surgery procedure lies in the weakening of the sclera with the micro-excisions, which leads to a level of increase in the natural accommodation amplitude. With the three dimensional model, the geometry of the sclera can be supplemented with the micro-excisions (holes). Fig. 7 and 8 show the position and the depth of the micro-excisions on the original geometry (*Hipsley and McDonald [2012]*). In my calculations, the initial material and geometrical properties are based on a 50 years old age-group, as *Hipsley and McDonald [2012]* made their laser procedure on patients with an average 50.4 years. The accommodation amplitude calculation is also performed on different geometries based on Fig. 9. The geometry on the right side of this figure has just theoretical significance because it is not applicable physiologically.

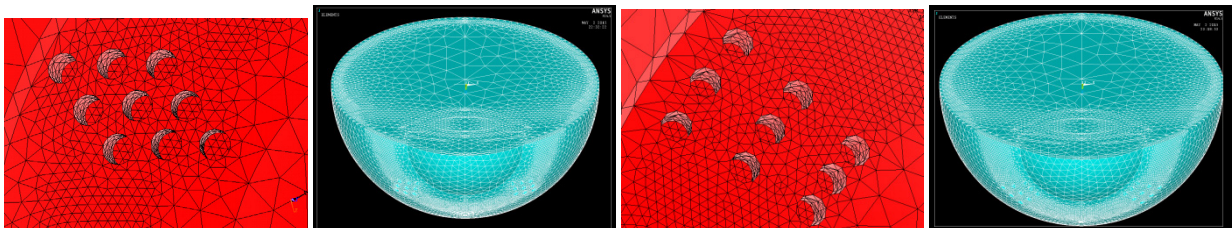


Figure 10 – The finite element mesh around the micro-excisions (original and the concentrated pattern)

For the sake of the comparability of the results, another calculation is performed where the stiffness of the sclera is neglected. It is also useful to prove the theoretical functioning of the surgery procedure. In Fig. 10 and 11 we can see the finite element mesh together with its refinement around the micro-excisions. For all the mentioned cases, the accommodation amplitude is calculated ( $\Delta COP$ ).

Table 1 – The detailed results in the different cases

Geometrical and material parameters in age 50 (n <sub>i</sub> =1,42; n <sub>a</sub> =1,336)	Intact	Original geometry	Concentrated holes	Continuous holes	Neglected sclera (intact)
COP (accommodated)	25,800 D	25,800 D	25,800 D	25,800 D	25,800 D
COP (unaccommodated)	23,859 D	23,785 D	23,783 D	23,764 D	22,519 D
ΔCOP	1,941 D	2,015 D	2,017 D	2,036 D	3,281 D
COP alteration respect to the intact state	0,000 D	0,07382 D	0,07622 D	0,09505 D	1,3397 D
change in lens thickness	0,2866 mm	0,2878 mm	0,288 mm	0,2897 mm	0,4282 mm
radius of curvature (anterior, accommodated)	8,706 mm	8,706 mm	8,706 mm	8,706 mm	8,706 mm
radius of curvature (anterior, unaccommodated)	10,821 mm	10,842 mm	10,838 mm	10,871 mm	11,861 mm
radius of curvature (posterior, accommodated)	5,031 mm	5,031 mm	5,031 mm	5,031 mm	5,031 mm
radius of curvature (posterior, unaccommodated)	5,090 mm	5,109 mm	5,110 mm	5,109 mm	5,323 mm

Table 1 contains the detailed results of the calculations together with the numerical results of the original geometry (*Hipsley and McDonald [2012]*). It can be seen that the increment in the accommodation amplitude is just about 0.1 D, which is only 6% of the average value what *Hipsley and McDonald [2012]* measured on their patients 1.5 years after the surgery. This difference can be originated from the fact that the applied material and geometrical parameters are based on only a few measurement groups.

Table 1 contains the results belong to the geometries of Fig. 9. From the concentrated holes column we can see that the amount of the volume obtained this way is the same as in the case of the original geometry, but with the concentrated holes geometry we can reach slightly larger accommodation amplitude than with the original one. As we expected, from the column that belongs to the continuous holes it can be concluded that the maximum increment in the accommodation amplitude can be reached in this case.

Based on my results, it can be said that the numerical model follows the tendency of the theoretical mechanism of the method.

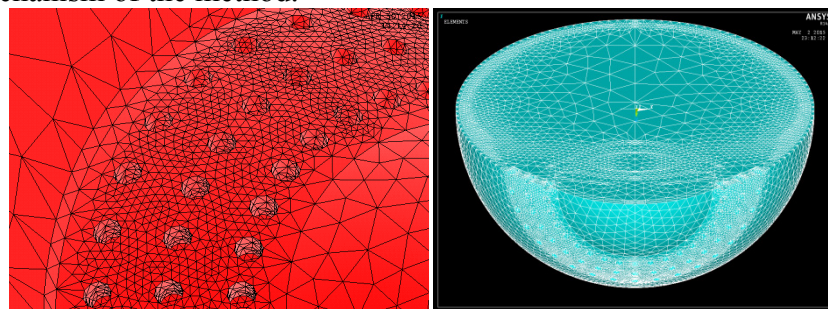


Figure 11 – The finite element mesh around the micro-excisions (continuous pattern)

The results of the complex model confirms the theoretical background of the technology. The continuous hole pattern leads to larger accommodation amplitude than the other analyzed hole pattern (Table 1). Last column of this table shows the results obtained by neglecting the sclera. Fundamentally, in this case the geometry and the material of the sclera do not affect the accommodation amplitude; its increment is 1.34 D. Of course, this result is not representative because in my model the role of the sclera cannot be ignored.

## 2.2 Experimental analysis of the zonular fibres

The mechanical behaviour of the zonular fibres play a major role in the mechanism of accommodation procedure. The force from the ciliary body is transferring to the lens through the zonular fibre system.

For the measuring of the mechanical parameters of these fibres – for example with tension tests – it is necessary to know the geometry (e.g. thickness and length parameters) of the bundles. After the analysis of the geometry of the zonular fibres with three different methods, a measurement procedure for the mechanical properties of the bundles have been developed together with two other methods for the evaluation of the Young's modulus of the zonules. Due to the anatomical similarity, porcine samples are used during the experiments.

### 2.2.1 Measurement of the zonular geometry

For the analysis of the network of porcine zonular fibres, scanning electron (SEM) and optical microscope are utilized, the second one in two different ways (OM I. and OM II.). Five-five eyeballs are used for the three analyses. The thickness of the zonular apparatus of each specimen is measured in four different positions where the bundles are parallel and their thickness are nearly the same. The lowest average thickness value has been measured with scanning electron microscope (SEM):  $33.2 \pm 9.1 \mu\text{m}$ . In case of the second method (OM I.) it is a bit thicker:  $43.2 \pm 9.6 \mu\text{m}$ , while at the third one (OM II.) the result is an average  $73.1 \pm 12.5 \mu\text{m}$  thickness for the bundles.

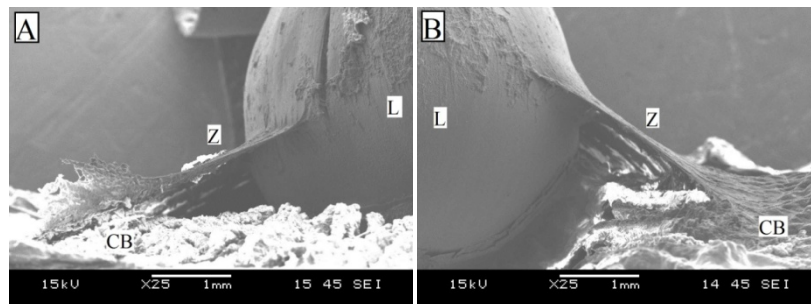


Figure 12 – SEM images about the zonular bundles, L – lens, Z – zonules, CB – ciliary body

### 2.2.2 Evaluation of the mechanical behaviour of the zonular fibres

For the investigations, thirty fresh porcine eyes were harvested from male animals (6-7 months old, 110-120 kg) from a local slaughterhouse. The samples were prepared and measured as quickly as possible to avoid any biological degradation, furthermore the ones with obvious deformation or damage were excluded from the study. The basic idea is to use three different sized prefabricated plastic rings for the measuring procedure (Fig. 13). Each ring had different purposes. Fig. 14 shows the preparation method of the samples.

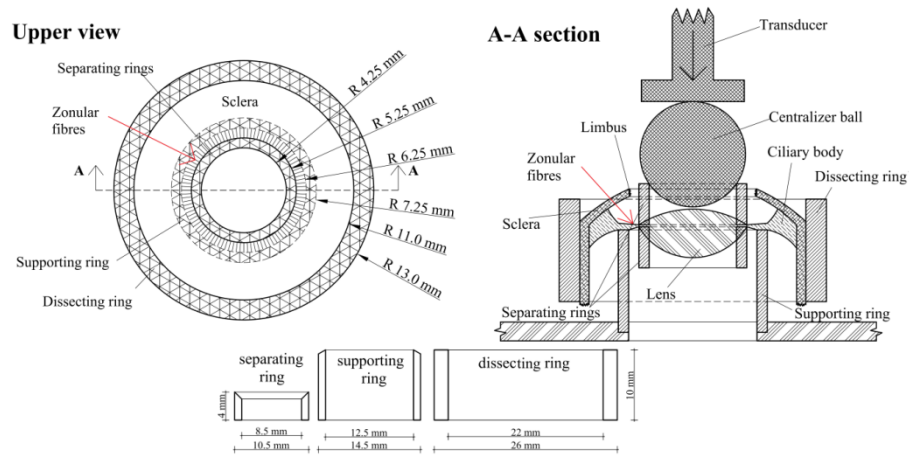


Figure 13 – Sketch of the measurement, and the section of the separating ring, the supporting ring and the dissecting ring

The tissues at the vicinity of the lens are removed, but the ciliary body, lens and zonular fibres remain intact (Fig. 14 F and I). The supporting ring excludes the effect of the ciliary body's elasticity, thus it is glued to the posterior side of the muscle with a thin (0.2 ml of cyanoacrylate) film layer (Fig. 14 J). Additionally, by gluing two separating rings to the lens (Fig. 13, Fig. 14 K-L) - also with a thin film layer (0.2 ml of cyanoacrylate) - the elasticity of the lens is excluded from the system. (Fig. 13, 14 K and L). Between the supporting ring and the separating rings, the zonular apparatus can be found in situ (Fig. 14 K). The transducer overlaid the upper separating ring (Fig. 13). A plastic centralizer ball is placed between the transducer and the specimen which ensures that the applied force is transferred in the vertical direction and in centralised form. During the loading procedure, the vertical translation of the transducer and the respective force are recorded continuously.

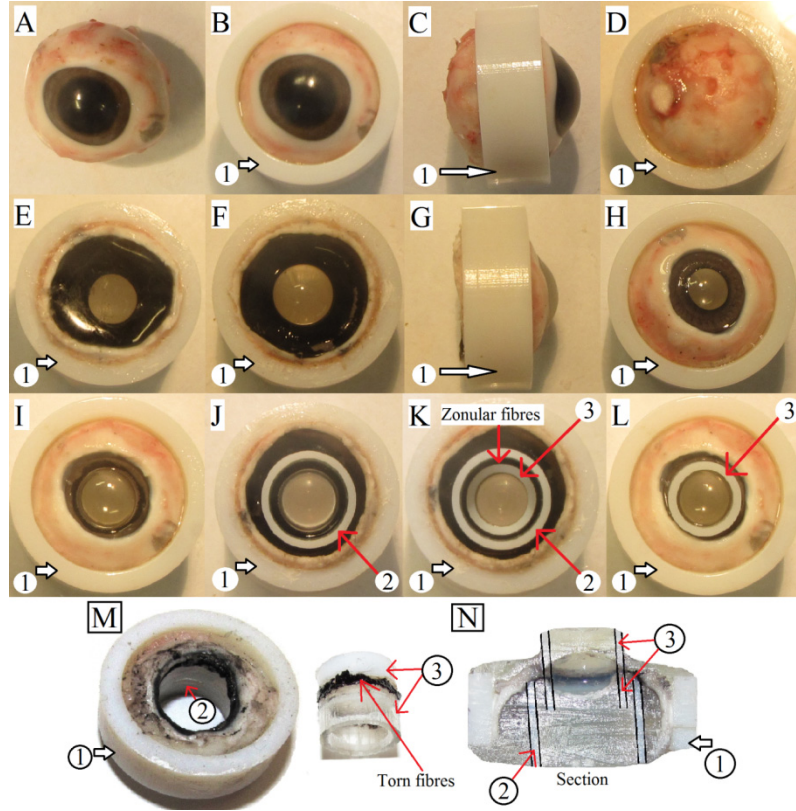


Figure 14 – Images of an experimental sample; upper view A, B, H, I, L; view from below D, E, F, J, K; side view C, G; specimen after a typical failure mode M; section view N; 1 – dissecting ring; 2 – supporting ring; 3 – separating ring

The equipment used (Z005, Zwick Roell AG, Ulm, Germany, material testing machine with  $10^{-5}$  N sensitivity, Zwick TestXpert 11.0 software) in the experiment is displacement-controlled during the measurements. The preload is 5 mN, the velocity of the transducer is 1 mm/min. At the initial stage the mass of the separating rings, lens and the centralizer ball can be calculated. By summing up these values, a total of ca.  $G=9$  mN initial force is received acting on the specimens resulting from their self-weight before the force-displacement recording. This specific value is very important at the comparison of the analytical solution and the finite element calculation with the laboratory tests (Fig. 15, where  $z_G$  is the displacement at  $G=9$  mN self-weight). To ensure the comparability, the analytical and the finite element results are need to be shifted according to Fig. 15. The following analytical solution can be used to determine the material parameters of the zonular fibres based on the results obtained from the laboratory tests. The material is assumed to be linear elastic and incompressible at the determination of the mechanical properties for the analytical solution. (See the detailed deduction in the dissertation.) The analytical solution (Fig. 15 B):

$$F(z) = 2R_i\pi E \frac{1}{2} \frac{z^2}{l_0^2} \frac{t_0(R_o - R_i)}{\sqrt{z^2 + l_0^2}} \frac{z}{\sqrt{z^2 + l_0^2}}, \quad (4)$$

where the force  $F(z)$  is a function of the vertical displacement,  $R_i$  is the outer radius of the separating ring,  $R_o$  is the inner radius of the supporting ring,  $l_0$  is the initial length of the zonular fibres,  $t_0$  is the initial thickness of the zonules,  $z$  is the vertical displacement,  $E$  is the Young's modulus of the zonules. With the help of Equation 4, the results of the laboratory tests are comparable with the analytical solution.

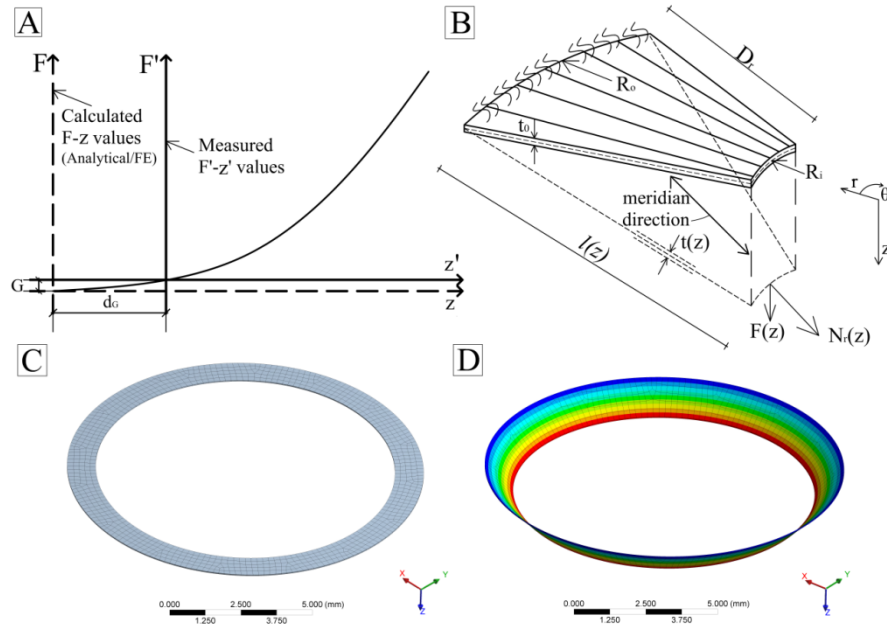


Figure 15 – The difference between the measured ( $F'-z'$ ) and calculated ( $F-z$ ) force-displacement diagrams (A); the notations on an infinitesimal element, “ss” means single supported edge,  $t$  is the thickness,  $l$  is the length of the fibres,  $D_r$  is the distance between the inner ( $R_i$ ) and outer ( $R_o$ ) radius,  $N_r$  is the normal force in the bundles (B); the mesh grid (C) and the total deformation of the computational finite element model (D).

For the finite element analysis, ANSYS Workbench 13.0 is used. For the mathematical approximation 8-node shell elements, for the geometrical approximation a plain ring with 10.5 mm inner and 12.5 mm outer diameters are used based on the experimental layout (Fig. 13). At the definition of the boundary conditions, simple supports are applied to the inner and outer edge, and a displacement load in normal direction to the plane of the ring at the inner edge (Fig. 15 D). During the calculation, the geometrical nonlinearity (effect of large displacements) is considered. Utilizing the results of the convergence analysis, the applied element number at the parametric study is set to about one thousand. The finite element calculation is made for the same purpose as the analytical solution, namely to evaluate the elastic parameters of the zonular fibres on macroscopic scale.

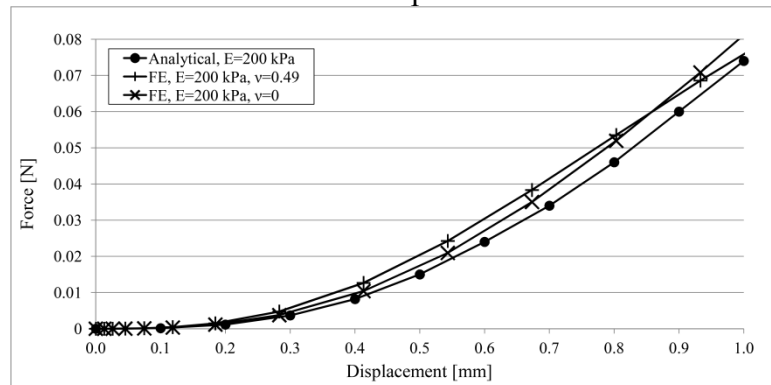


Figure 16 – The analytical solution compared with the FE calculations;  $E$  is the Young's modulus,  $\nu$  is the Poisson's ratio

With the help of the Poisson's ratio, the transverse effect of the fibres are studied, because the zonules are actually not completely individual fibres, they are interlaced and exhibit some uncertain transverse connections and interactions between each other in circumferential direction. The  $\nu=0$  Poisson's ratio considers the complete individuality, and the  $\nu=0.49$  value models some connections between the neighbouring fibres. In the finite

element calculation an initial stress is also taken into account, based on the presumable fact that three hours after the slaughtering the ciliary muscle is in rigor mortis state, and according to this condition, the zonular bundles are almost relaxed during the preparation.

Fig. 17 shows the measured force-displacement diagrams from the beginning until material failure. The load applied to the specimens is a monotonically increasing force, but it has a cyclic period at the initial stage of the loading procedure in order to settle the system. Fig. 14 M shows a sample specimen after a typical failure at the end of the test. Fourth order polynomial regressions are applied to all of the measured force-displacement relations of the specimens in the 0 to 1 mm interval of the vertical displacement field (Fig. 16 and 17). The mean curve has zero force values under 0.07 mm displacement. This effect can be explained by the fact that the system is settled and the disturbances caused by the uncertainty of the support, the abutting parts, etc., during unloading and reloading are excluded in this way. The standard deviations of the measured forces are calculated at discrete displacements (Fig. 17) in a very easy way due to the fitting method. The laboratory test results and the analytical solution are comparable using Equation 4. Fig. 18 shows the mean result and standard deviation of the laboratory tests together with the analytical solutions calculated with values for the Young's modulus ranging between 100-350 kPa with 50 kPa steps. The graph shows that according to the laboratory measurements, the Young's modulus of zonular bundles is in the 150-250 kPa range. Fig. 19 shows the results of the FE parametric study with and without initial stresses in the zonules. According to it, the assumed values for the initial stresses seem reasonable, because when we consider their effect, we receive  $E \approx 200$  kPa Young's modulus that describes the elastic behaviour of the zonular bundles very accurately. The purposes of our study were to devise an appropriate complex laboratory test method to evaluate the mechanical behaviour of zonular bundles in situ and to determine the macroscopic elastic mechanical parameters of these bundles based on the results.

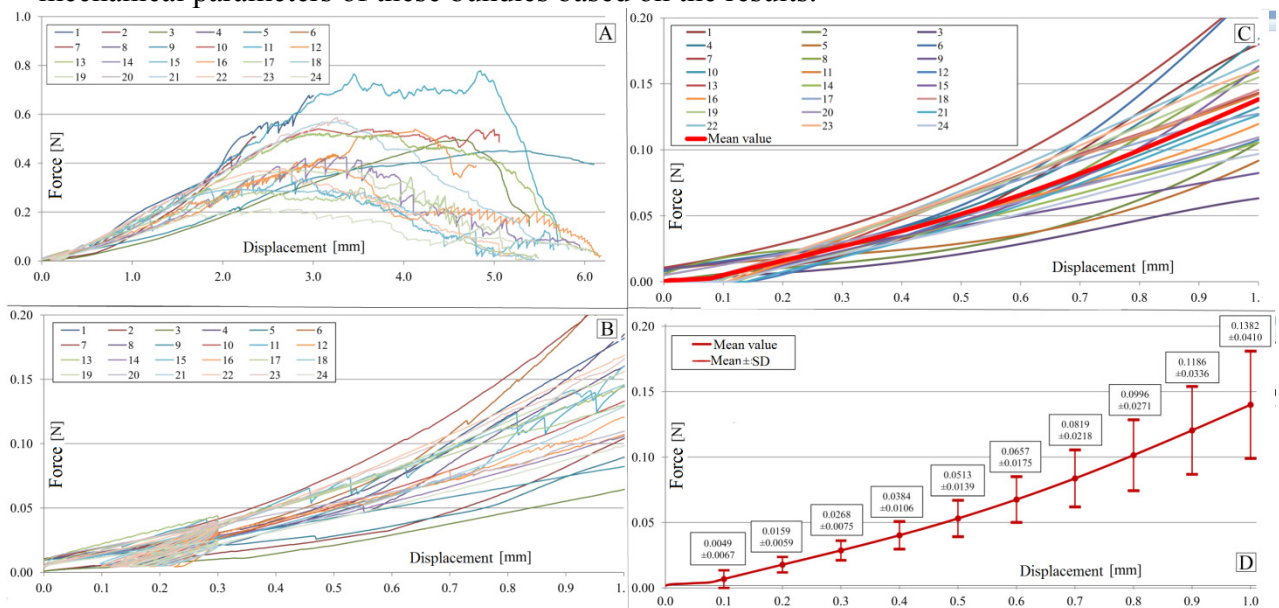


Figure 17 – The measured force-displacement diagrams of the laboratory tests (A); the initial interval of the measured force-displacement diagrams (B); The 4<sup>th</sup> order polynomial regressions (C) and the mean value with the standard deviations at characteristic displacements (D)

According to the analytical and the finite element solutions, the Young's modulus of the zonular bundles is around 200 kPa. Fig. 16 shows that the Poisson's ratio and the initial stresses have only a slight effect on the force-displacement diagram. According to our best knowledge, the current study is the first that determines the Young's modulus for porcines. Therefore, a direct mechanical comparison is not possible for our current result. Additionally,

these results come from a completely intact measurement with respect to the zonules, which significantly differs from the other measurements. Furthermore, we emphasize that the aim of our study was to develop such a method, which is able to determine the Young's modulus of zonular fibres in situ. In our opinion, the method presented in this paper is accurate, reliable, and can be adapted to human eyes.

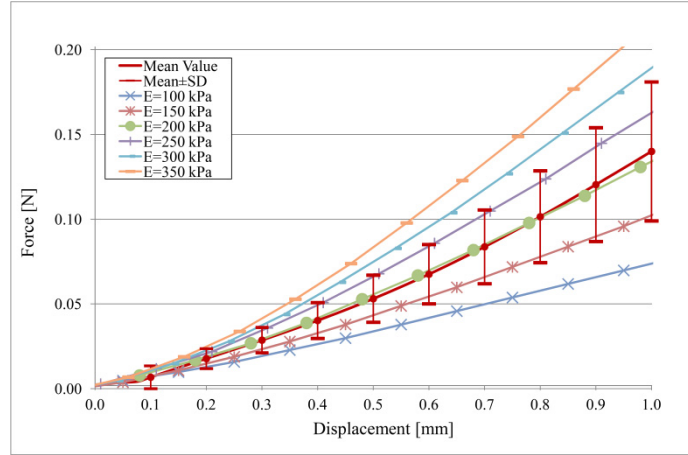


Figure 18 – The analytical solutions compared with the mean±SD values of the laboratory tests;  $E$  is the Young's modulus.

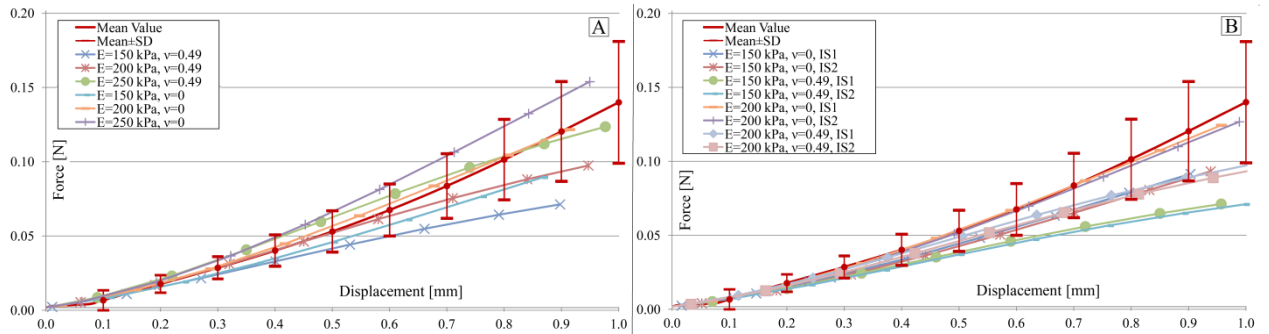


Figure 19 – The results of the FE analysis compared with the mean±SD values of the laboratory tests;  $E$  is the Young's modulus,  $\nu$  is the Poisson's ratio (A); The effects of the initial stresses and Poisson's ratios compared with the mean±SD values of the laboratory tests;  $E$  is the Young's modulus,  $\nu$  is the Poisson's ratio,  $IS1=4.4$  kPa and  $IS2=8.4$  kPa are the two different initial stress values (B)

### **3. New scientific results**

I summarized my results in the following five theses:

#### ***Thesis 1***

*I created a complex eyeball finite element model. The specific ophthalmic geometry and material properties of the model can be arbitrarily modified. Based on the input geometrical parameters the model is generated automatically. The complex model can be widely used to analyze different ophthalmic problems with the follow-up of the deformation and internal forces of each component. The model contains every important part from biomechanical point of view. I tested the usability of the complex model with the analysis of the accommodation. I compared the received outcomess with other authors' results and pointed out the advantages of my model. [4, 7, 10]*

#### ***Thesis 2***

*I analyzed the effect of changing of geometrical, mechanical and optical parameters respect to the age on the accommodation amplitude of the lens with the developed finite element model. For this calculation, I defined the central dioptré power of the lens in more precise way than in the former publications. With the help of the numerical model, I proved a hypothesis raised among ophthalmologists, namely that the effect of the refractive index plays at least as much role than the geometrical and mechanical parameters of the lens on the altering of the accommodation amplitude of the lens due to ageing. [4, 6, 9]*

#### ***Thesis 3***

*With the application of the complex finite element model I analyzed a patented surgery method (related to the sclera) developed to restore the accommodation amplitude of the eye. I verified the effect of the surgical procedure on the accommodation and the principle of its functioning. I did a parametric study that helped to determine the effects of the layout and the amount of the holes formed during the surgery on the accommodation amplitude. Based on the results of the numerical model I suggested a physiologically possible new layout of the geometry that results greater increment in the accommodation amplitude than the original geometry. [4, 6]*

#### ***Thesis 4***

*I developed a new individual laboratory method to characterize the elastic constants of the zonular fibres. The complete method is reproducible with simple laboratory tools. The first goal of the method was to keep the zonular bundles in-situ position during the sample preparation. Thus, the insertions of the zonules on the lens and on the ciliary body were intact. During the measurements the elasticity of the zonules were separated, namely the elastic contribution of the surrounding parts is excluded. Furthermore, the second goal was to apply the most simple force transfer between the transducer and the sample to reach the most precise results for the evaluation. I tested the measuring procedure on porcine samples, therefore the porcine zonular geometry was obtained with different methods. [1, 5]*

#### ***Thesis 5***

*I deduced an analytical solution to evaluate the Young's modulus of the zonular apparatus based on the laboratory tests, which provides the range of this material constant in a simple way. I verified the applicability of the analytical solution with a finite element parametric study. [1, 5]*

## **Publication on the subject of the dissertation**

### **International journal papers**

- [1] Bocskai, Z.I., Sándor, G.L., Kiss Z., Bojtár, I., Nagy, Z.Z. (2014): Evaluation of the mechanical behaviour and estimation of the elastic properties of porcine zonular fibres. *Journal of Biomechanics*, 47(13), pp. 3264-3271. (IF 2,496)
- [2] Sándor, G.L., Kiss, Z., Bocskai, Z.I., Kolev, K., Takács, Á.I., Juhász, É., Kránitz, K., Tóth, G., Gyenes, A., Bojtár, I., Juhász, T., Nagy, Z.Z. (2014): Comparison of the mechanical properties of the anterior lens capsule following manual capsulorhexis and femtosecond laser capsulotomy, *Journal of Refractive Surgery*, 30, pp. 660-664. (IF 2,781)
- [3] Sándor, .L., Kiss, Z., Bocskai, Z.I., Kolev, K., Takács, Á.I., Juhász, É., Kránitz, K., Tóth, G., Gyenes, A., Bojtár, I., Juhász, T., Nagy, Z.Z. (2015): Evaluation of the mechanical properties of the anterior lens capsule following femtosecond laser capsulotomy at different pulse energy settings, *Journal of Refractive Surgery*, 31, pp. 153-157. (IF 2,781)

### **Hungarian journal papers in English**

- [4] Bocskai, Z.I., Bojtár, I. (2013): Biomechanical modelling of the accommodation problem of human eye. *Periodica Polytechnica – Civil Engineering*, 57(1), pp. 3-9. (IF 0,250)
- [5] Bocskai, Z.I., Kiss, Z., Sándor, G.L., Bojtár, I., Nagy, Z.Z. (2014): Scanning electron and optical microscopic studies of the system of porcine zonular fibres, *Biomechanica Hungarica*, 7(2), pp. 5-11.

### **Hungarian journal papers in Hungarian**

- [6] Bocskai, Z.I., Bojtár, I.: Az ínhártyát érintő lézeres látásjavító szemműtét végeeselemes vizsgálata és elemzése, *Biomechanica Hungarica*, 8(2), (közlésre elfogadva)

### **Book chapters**

- [7] Bocskai, Z.I., Bojtár, I. (2012): Emberi szem biomechanikai vizsgálata. In Kiss R.M. (szerk.), *Biomechanikai modellezés, monográfia*, TERC Kereskedelmi és Szolgáltató Kft., Budapest, ISBN 978-963-996-840-0, pp. 187-202.
- [8] Sándor, G.L., Kiss, Z., Bocskai, Z.I., Bojtár, I., Takács, Á.I., Nagy, Z.Z. (2014): Mechanical behavior of capsulotomy performed with femtosecond laser. In: Nagy, Z.Z., (szerk.), *Femtosecond laser-assisted cataract surgery: facts and results*, Slack Incorporated, Thorofare, ISBN 978-1-61711-996-5, pp. 29-31.

### **Conference papers in English**

- [9] Bocskai, Z.I. (2012): Numerical simulation of the human eye accommodation. *Proceedings of the Conference of Junior Researchers in Civil Engineering*, Budapest, Hungary, 19-20 June, ISBN 978-963-313-061-2, pp. 17-22.

### **Conference papers in Hungarian**

- [10] Bocskai, Z.I., Bojtár, I. (2011): Az emberi szem biomechanikai modellezése. *Építőmérnöki Kar a Kutatóegyetemért*, monográfia, kiadja az BME Építőmérnöki Kar dékánja, Budapest, ISBN 978-963-313-042-1, pp. 73-78.

## Conference presentation

- [11] Bocskai, Z.I., Bojtár, I. (2012): Szemészeti problémák modellezése végeelem módszer alkalmazásával. *SHIOL – Societas Hungarica Ad Implantandum Oculi Lenticulam, Magyar Műlencse és Refraktív Sebészeti Társaság Kongresszusa*, Budapest, Magyarország, március 29-31., pp. 34.
- [12] Bocskai, Z.I., Bojtár, I. (2012): The complex biomechanical analysis of the human eye, *ESMC-2012 – 8th European Solid Mechanics Conference*, Graz, Austria, 9-13 July, ISBN 978-3-85125-223-1, pp. 1-2.
- [13] Bocskai, Z. I., Bojtár, I. (2013): A szemlencse és környező részeinek mechanikai viselkedése. *V. Magyar Biomechanikai Konferencia*, Budapest, Magyarország, május 24-25., pp. 55.
- [14] Bocskai, Z.I., Kiss, Z., Sándor, G.L., Bojtár, I., Nagy, Z.Z. (2013): Measurement of porcine zonular fibres. *Euromech Colloquium 533, Biomechanics of the Eye*, University of Genoa, Italy, 22-24 July, pp. 39-40.
- [15] Bocskai, Z.I., Bojtár, I. (2014): A LaserACE eljárás hatékonyságának biomechanikai elemzése a dinamikus akkomodáció növelése érdekében. *A Magyar Szemorvostársaság 2014. évi Kongresszusa*, Pécs, Magyarország, június 26-28. *Szemészet*, 151, supplementum I., ISSN 0039-8101, pp. 30.

## Seminar lecture

- [16] Bocskai, Z.I., Bojtár, I. (2011): Biomechanical modelling of the human eye. *18th Inter-Institute Seminar for Young Researchers*, Budapest, Magyarország, 23-25 September, pp. 15.
- [17] Bocskai, Z.I., Bojtár, I. (2012): A presbyopia új excimer lézeres javíthatósága: akkomodáció és presbyopia a mérnök szemével – modellezés végeelem módszer segítségével. *SHIOL – Societas Hungarica Ad Implantandum Oculi Lenticulam, Magyar Műlencse és Refraktív Sebészeti Társaság Kongresszusa*, Budapest, Magyarország, március 29-31.
- [18] Bocskai, Z.I., Kiss, Z., Sándor, G.L., Bojtár, I., Nagy, Z.Z. (2013): Measurement of porcine eye zonular fibres. *19th Inter-Institute Seminar for Young Researchers*, Institute for Mechanics of Materials and Structures, Vienna, Austria, 11-12 October, ISBN 978-3-9503537-2-3, pp. 21.

## References in the booklet

- Chien, C.H., Huang, T., Schachar, R.A. (2003): A mathematical expression for the human crystalline lens, *Comprehensive Therapy*, 29, pp. 244-258.
- Hipsley, A., McDonald, M. (2012): Laser Scleral Matrix Microexcisions (LaserACE/Erbium YAG Laser), In: Pallikaris I., Plainis S., Charman W.N. (editors): *Presbyopia, Origins, Effects and Treatment*, SLACK Incorporated, pp. 219-223.
- Śródka, W. (2011): Evaluating the material parameters of the human cornea in a numerical model, *Acta of Bioengineering and Biomechanics*, 13, pp. 77-85.
- Tsorbatzoglou, A., Németh, G., Széll, N., Biró, Z., Berta, A. (2007): Anterior segment changes with age and during accommodation measured with partial coherence interferometry, *Journal of Cataract and Refractive Surgery*, 33, pp. 1597–1601.